Solution Structure by 2D ^{1}H-NMR of a Chimeric Peptide Recognized by Galanin and Neuropeptide Y Receptors†

Klas Arvidsson,‡ Tiit Land,‖ Ülo Langel,‖ Tamas Bartfai,‖ and Anders Ehrenberg*,‡

Departments of Biophysics and Neurochemistry & Neurotoxicology, Arrhenius Laboratories, Stockholm University, S-106 91 Stockholm, Sweden

Received March 2, 1993; Revised Manuscript Received April 27, 1993

ABSTRACT: The 25 amino acid residue chimeric peptide M32, galanin(1–13)–neuropeptide Y(25–36)-amide, was synthesized. The peptide was found to be recognized by both galanin and NPY receptors. The solution structure in 30% (v/v) 1,1,1,3,3,3-hexafluoro-2-propanol was examined by 2-D ^{1}H-NMR and by CD. Proton resonance assignments were made, and structures were calculated using DIANA and refined by restrained energy minimization and molecular dynamics. The obtained structures contain an α-helical part in the NPY portion of the peptide including residues 13–20, and in some structures it continues to the C-terminal Tyr25. The more flexible N-terminal portion of the peptide has the freedom to approach the C-terminal α-helix, via a reverse turn or a nascent α-helix, which permits the N-terminus with Trp2 to come into close contact with the C-terminus with Tyr25. Among the ten NMR structures with lowest energy, there are structures reminiscent of the horseshoe shape of aPP, a close relative of NPY with known crystal structure. It appears that the strong α-helical character of the NPY(25–36)amide fragment of M32 helps to stabilize structural features in the galanin-derived part of the peptide. It is noteworthy that this rigid NPY portion of M32 does not prevent the recognition of the peptide by galanin receptors; rather, the peptide has unusually high affinity: $IC_{50} = 0.1$ nM at galanin receptors. The chimeric peptide M32 is also recognized by NPY receptors with submicromolar affinity ($IC_{50} = 0.25$ μM). The availability of a solution structure for peptide M32, which is recognized by two peptide receptors that are both members of the family of G-protein-coupled receptors, may be useful in understanding peptide receptor–ligand interactions and in designing new galanin and NPY receptor ligands.

Chimeric peptides composed of biologically active fragments of different neuropeptides often display interesting properties different from those of the isolated fragments. In some cases it has been found that the affinity for the respective receptors is dramatically enhanced (Gozes et al., 1991; Bartfai et al., 1991). In addition, it has been shown in biological tests that such chimeric peptides may act as antagonists on at least one of the two corresponding peptide receptors (Bartfai et al., 1991, 1992; Gozes et al., 1991; Lindskog et al., 1992; Wiesenfeld-Hallin et al., 1992). The structural basis for the high affinity of such chimeric peptides at two receptors and for their action as antagonists is not understood. Improved knowledge on this point would form a basis for attempts to construct nonpeptide compounds with similar properties.

In the present study we describe the synthesis of the chimeric peptide galanin(1–13)–NPY(25–36)amide, i.e., GWTLN-SAGYLLGPRHYINLITRQRY-NH_2, investigate the binding properties of this peptide to galanin and NPY[1] receptors, and determine the possible solution structures adopted by this chimeric peptide on the basis of CD and ^{1}H-NMR experiments. The particular composition of this chimeric peptide was based on earlier investigations of receptor binding properties of fragments of galanin (Land et al., 1991a) and NPY (Abens et al., 1989) and experiences with chimeras from galanin and substance P or bradykinin. The structure–function analysis of the present galanin–NPY chimera will benefit from existing structural studies on galanin and NPY and their fragments.

Studies on galanin fragments have shown that at least the sequence of residues 1–12 of galanin is required for recognition of the peptide by galanin receptors (Land et al., 1991a). All the N-terminal fragments 1–12, 1–15, and 1–16 of galanin are high-affinity agonists in biological test systems (Fisone et al., 1991). The chimeras galanin(1–13)–substance P(5–11)-amide and galanin(1–13)–bradykinin(2–9)amide show high-affinity binding to galanin receptors (Bartfai et al., 1991; Langel et al., 1992; Wiesenfeld-Hallin et al., 1992) and function as antagonists toward the galanin receptor responses (Bartfai et al., 1991; Lindskog et al., 1992; Wiesenfeld-Hallin et al., 1992; Bartfai et al., 1992). Hence also the present chimeric peptide was constructed with the N-terminal portion identical to the galanin sequence 1–13.

Investigations have been made with NPY fragments binding to NPY receptors in membranes from rat cerebral cortex and in the human neuroblastoma cell line SK-N-BE2. It was found that for recognition at the receptor the minimal C-terminal fragments were the sequences 19–36 (Abens et al., 1989) and 22–36 of NPY (Wahlestedt et al., 1990),

† This work was supported by grants from the Swedish Natural Science Research Council, the Magn. Bergvall Foundation, the Carl Trygger Foundation for Scientific Research, the Erna and Victor Hasselblad Foundation, the Wenner-Gren Foundation, and the Board of Technical Development (STU/NUTEK).

* To whom correspondence should be addressed.

‡ Department of Biophysics.

‖ Department of Neurochemistry & Neurotoxicology.

[1] Abbreviations: aPP, avian pancreatic polypeptide; bPP, bovine pancreatic polypeptide; NPY, neuropeptide Y; NMR, nuclear magnetic resonance; 2-D, two-dimensional; COSY, correlated spectroscopy; DQF, double quantum filtered; RELAYED-COSY, relayed coherence transfer spectroscopy; NOE, nuclear Overhauser enhancement; NOESY, NOE spectroscopy; ROESY, rotating frame NOE spectroscopy; TOCSY, total correlation spectroscopy; FID, free induction decay; DIANA, distance geometry algorithm for NMR applications; REDAC, redundant dihedral angle constraints; rEM, restrained energy minimization; rMD, restrained molecular dynamics; M32, galanin(1–13)–NPY(25–36)amide.

0006-2960/93/0432-7787$04.00/0

respectively. There is also another NPY receptor subtype, which for recognition of the peptide requires the N-terminal residues 1–4 of NPY as well as the C-terminal sequences 25–36 (Schwartz et al., 1989; Wahlestedt et al., 1990; Rivera & Undén, 1990; McLean et al., 1990). Since the shortest significant C-terminal portion of NPY is the sequence 25–36, we have selected this for the C-terminal section of the chimeric peptide with galanin.

The solution structure of galanin, a 29-residue peptide, has been studied by ^{1}H-NMR in more than one solvent. Wennerberg et al. (1990) have reported that galanin in neat 2,2,2-trifluoroethanol adopts a predominantly α-helical structure. We have found (K. Arvidsson et al., unpublished results) that, in 30% (v/v) 1,1,1,3,3,3-hexafluoro-2-propanol, galanin has only about 30% as large a tendency to form α-helix structure. N-terminal fragments, galanin(1–16) and shorter ones, did not show any appreciable tendency to form α-helix structure even in neat 2,2,2-trifluoroethanol as deduced from CD measurements (K. Arvidsson, unpublished results).

NPY is a 36-residue neuropeptide which was discovered by Mutt and co-workers, as was galanin (Tatemoto et al., 1982, 1983). It is a member of the family of homologous pancreatic polypeptides which occupies a unique position among neuropeptides, since the structure of one of the members, avian pancreatic polypeptide, aPP, also consisting of 36 residues, has been solved by X-ray crystallography (Blundell et al., 1981). These results reveal that aPP is like a small protein with a horseshoe shape, where an N-terminal stretch of polyproline residues 1–8 runs antiparallel to a C-terminal α-helix of ca. five turns, thus bringing the two ends of the peptide close to each other. By analogy, similar proximity between the N- and the C-terminus has been inferred to be present in NPY (Allen et al., 1987; MacKerell, 1988; Schwartz et al., 1989). In aqueous solutions similar structures have been determined from ^{1}H-NMR data for human NPY (Darbon et al., 1992) and for bovine pancreatic polypeptide, bPP (Li et al., 1992). In several other cases ^{1}H-NMR investigations of NPY in water (Saudek & Pelton, 1990; Cowley et al., 1992), in neat 2,2,2-trifluoroethanol (Mierke et al., 1992), and in 30% (v/v) 1,1,1,3,3,3-hexafluoro-2-propanol (K. Arvidsson et al., unpublished results) show a well-developed C-terminal α-helix. However, no NOE contacts suggesting a stabilized back folding of the polyproline N-terminal section are found.

The isolated C-terminal fragment NPY(13–36)amide and several analogues thereof have also been studied by ^{1}H-NMR in 30% (v/v) 1,1,1,3,3,3-hexafluoro-2-propanol (K. Arvidsson et al., unpublished results). The results, to be reported elsewhere, show that the C-terminal α-helix of NPY is quite robust. Results of CD studies (K. Arvidsson et al., unpublished results; Ishigura et al., 1988) point in the same direction.

MATERIALS AND METHODS

Peptide Synthesis

The peptides were synthesized in a stepwise manner on a solid support using an Applied Biosystems Model 431A peptide synthesizer with the standard *N*-methylpyrrolidone/hydroxybenzotriazole (HOBt) solvent-activation strategy on a 0.1-mmol scale. We used *tert*-butyloxycarbonyl (*tert*-BOC) amino acids which were coupled to *tert*-BOC amino acid phenylacetamidomethyl resin (Nova Chemical Company Ltd., U.K.) or *p*-methylbenzhydrylamine resin (Bachem Feinchemikalien AG, Switzerland) as HOBt esters. All solvents and all other reagents for automatic peptide synthesis were from Applied Biosystems. The reagent used in the deprotection and cleavage steps were of analytical grade and used without further purification. The peptides were cleaved from the resin, deprotected, and purified as described earlier (Land et al., 1991a). The purity of the product was checked by analytical HPLC. Molecular weights of the peptides were determined using plasma desorption mass spectrometry (PDMS) (Model Bioion 20, Applied Biosystems).

Receptor Binding

Preparation of [^{125}I]Monoiodo-Tyr^{26}-porcine Galanin. Synthetic porcine galanin(1–29) was iodinated with Na^{125}I (NEN, Boston, MA) by the chloramine-T method to yield [^{125}I]monoiodo-Tyr^{26}-porcine galanin (specific activity 1800–2000 Ci/mmol), as described by Land et al. (1991b), and was used in ligand binding studies carried out at equilibrium.

Preparation of Membranes. The tissue homogenates of rat hypothalami or cerebral cortex were prepared as described by Land and co-workers (1991b). The membranes were resuspended in bacitracin-containing (1 mg/mL) 5 mM Hepes-buffered Krebs–Ringer solution (137 mM NaCl, 2.68 mM KCl, 1.8 mM $CaCl_2$, and 1 g/L glucose) at pH 7.4 and used immediately in equilibrium binding experiments.

Displacement of [^{125}I]Galanin and [^{3}H]NPY by Their Receptor Ligands. Displacement experiments were carried out in bacitracin-containing (1 mg/mL) 5mM Hepes-buffered Krebs–Ringer solution, with 0.05% (w/v) bovine serum albumin (pH 7.4) in the presence of 0.2 nM [^{125}I]galanin or 0.1 nM [^{3}H]NPY (Amersham, U.K.). These experiments and the addition of increasing concentrations (10^{-12}–10^{-6} M) of unlabeled porcine galanin, NPY, or the substance to be tested were carried out as described earlier (Land et al., 1991b). The IC_{50} values of the displacing ligands were calculated by fitting the experimental data using a nonlinear least squares method, using the program KaleidaGraph on a Macintosh SE.

Circular Dichroism

CD measurements were carried out on a Jasco J-720 spectropolarimeter at Kabi Pharmacia Biopharma at 22 °C, using a 1.0-nm bandwidth, a scanning rate of 10 nm/min with a wavelength step of 0.2 nm, and a time constant of 2 s. Each spectrum was an accumulation of two scans over the range 190–250 nm with a light path length of 2 mm for both sample and solvent.

Samples were prepared in H_2O with 20 mM acetic acid and five different concentrations of 1,1,1,3,3,3-hexafluoro-2-propanol: 0, 10, 20, 30, and 40% (v/v). The peptide concentration at 0% 1,1,1,3,3,3-hexafluoro-2-propanol was determined to 40 μM by UV light absorption measurements. The maximum specific absorptivity of the peptide, ϵ_{276nm} = 9532 L mol^{-1} cm^{-1}, was obtained using tabulated values for the free amino acids in aqueous solution (Sober, 1970), considering that the peptide contains one Trp and three Tyr residues. The CD spectra recorded in the presence of 1,1,1,3,3,3-hexafluoro-2-propanol were corrected for dilution effects.

NMR Spectroscopy

Sample Preparation. Lyophilized material, i.e., purified peptide with counter ions, was dissolved in 20 mM deuterated acetic acid in H_2O in the presence of 30% (v/v) deuterated 1,1,1,3,3,3-hexafluoro-2-propanol to a peptide concentration of approximately 1.5 mM. The sample contained 10% ^2H_2O for locking and 0.25 mM of the sodium salt of 3-(trimeth-

ylsilyl)-[3,3,2,2-^{2}H]propionic acid, which served as an internal chemical shift reference. The pH meter reading was 3.1, uncorrected. Another sample with pH 4.2 was prepared by adding a small amount of triethanolamine. A ^2H_2O sample with 30% (v/v) 1,1,1,3,3,3-hexafluoro-2-propanol, 20 mM deuterated acetic acid, and uncorrected p^{2}H 3.3 was prepared to give a peptide concentration of approximately 3 mM.

NMR Experiments. Most 2-D NMR experiments were recorded on a JEOL GX-400 spectrometer. A series of 2-D TOCSY spectra and a 2-D ROESY spectrum were recorded on a JEOL JNM-A400 spectrometer, and a 2-D NOESY and a 2-D ROESY spectrum were recorded on a Varian Unity 600 spectrometer. The two-dimensional spectra were collected in the pure phase absorption mode according to the method of States et al. (1982). Sets of standard (Wüthrich, 1986) 2-D DQF-COSY and NOESY (mixing time 250 ms) spectra were accumulated at 15, 30, and 50 °C at pH 3.1, and another set were accumulated at 30 °C, pH 4.2. At 15 °C and pH 3.1, 2-D RELAYED-COSY experiments (Eich et al., 1982) were accumulated with mixing times of 25 and 70 ms. Solvent signal suppression was achieved by presaturation. A relaxation delay of 1.5 s was used. The transmitter offset was placed on the H_2O resonance. Elimination of baseline artifacts was achieved by optimizing the "receiver-on" time and the "in-phase" time (Hoult et al., 1983; Davis, 1989).

Typically, data were collected after 4 dummy scans with 96 or 128 added free induction decays, 1024 data points in the t_2 dimension, and 256 increments in the t_1 dimension. The spectral width was 5 kHz. In the DQF-COSY experiments a convolution difference apodization function with line broadening of 20 Hz and a trapezoidal weighting function were applied to each free induction decay prior to Fourier transformation. The NOESY free induction decays were subjected to a 10° shifted sine-bell, an exponential multiplication with 3-Hz broadening, and a trapezoidal function in each dimension. Zero-filling was applied once in each dimension, giving 2048 and 1024 data points in the t_2 and t_1 dimensions, respectively, leading to a digital resolution of 4.88 Hz/point in both F_1 and F_2.

A highly resolved DQF-COSY spectrum with 4096 data points in the t_2 dimension and 256 in the t_1 dimension was recorded to enable the determination of $^3J_{HN\alpha}$ spin–spin coupling constants, using the method proposed by Kim and Prestegard (1989). Slices through each resolved antiphase fingerprint cross peak were extracted. In order to increase the final digital resolution of the one-dimensional slices, complex free induction decays were regained by applying Hilbert transformation and inverse Fourier transformation. After zero-filling three times, a trapezoidal apodization function was applied prior to Fourier transformation. The final digital resolution was 0.30 Hz/point.

In order to determine the amide proton exchange rates in M32, a series of 2-D TOCSY experiments, with a mixing time of 30 ms, were recorded at 15 °C on a fresh ^2H_2O sample. Four FIDs were added for each of the 200 time increments in the t_1 dimension. In the t_2 dimension 2048 data points were collected. The spectral width was 5 kHz. A pulse delay of 1.0 s was used, giving a total acquisition time of 33 min for each 2-D TOCSY experiment. The apodization functions applied were the same as in the NOESY experiments. Zero-filling was performed in both dimensions, giving a digital resolution of 1.22 and 4.88 Hz/point in the F_2 and F_1 dimensions, respectively.

The NMR spectra were processed either on a Convex C-2 mini supercomputer using the FTNMR software (Hare Research Inc.) or on a Silicon Graphics Personal Iris 4D25TG workstation using the FELIX software (Biosym Technologies Inc.).

Structure and Dynamics Calculation

NMR Derived Restraints. Strong-, medium-, and weak-intensity NOESY cross peaks were transformed into upper distance limits of 0.27, 0.33, and 0.50 nm, respectively (Nilges et al., 1988). The peak intensities were estimated by counting the number of contour levels in the NOESY spectrum.

No stereospecific assignments could be made directly from the NOE intensities.

Dihedral ϕ angle restraints were obtained from $^3J_{HN\alpha}$ spin–spin coupling constants (Bystrov, 1976), using an empirically determined (Pardi et al., 1984) Karplus equation (Karplus, 1959).

Distance Geometry. Structures were initially generated using the program DIANA including REDAC (Güntert et al., 1991; Güntert & Wüthrich, 1991). In order to more completely sample the conformation space consistent with the applied restraints, the DIANA structures were subjected to restrained energy minimization, rEM, and restrained molecular dynamics, rMD, using the program DISCOVER from Biosym Technologies Inc. Finally, rEM was performed on selected snapshots from the rMD calculations, in order to refine the geometry of these structures as well as to decrease the internal strain contained in them. All DIANA, rEM, and rMD calculations and analysis of structures were performed on a Silicon Graphics Personal Iris 4D25TG work station.

Upper distance restraints were modified by DIANA so as to simultaneously allow for both possible stereospecific assignments of diastereotopic substituents, resulting in the introduction of pseudoatoms for methylene protons and methyl groups. Restraints on aromatic side-chain protons were manually modified according to the standard pseudoatom representation (Wüthrich et al., 1983).

In order to avoid incorrect emphasis of the energy terms of atoms close in space, the force constant of the explicit lower distance limit restraints was 0 in the structure calculations. No explicit hydrogen bond restraints were included in the structure calculations.

A total of 30 DIANA structures were calculated using the standard minimization parameters (Güntert & Wüthrich, 1991), resulting in calculations over nine levels.

The ϕ-angle restraints calculated from the measured $^3J_{HN\alpha}$ and all upper distance restraints deduced from the NOESY spectra were used as starting input parameters for the DIANA calculations. The list of distance restraints was modified by the DIANA program, which deleted the redundant ones. The DIANA calculations were carried out by going through four REDAC cycles, which introduced new dihedral angle restraints, of which about half applied to the polypeptide backbone. No new such restraints were introduced by the last REDAC processing. The final DIANA refinement was performed on each of these structures using all nonredundant distance restraints and the initially introduced dihedral ϕ angle restraints.

Structure Refinement by rEM and rMD. The further refinement protocol consisted of two steps of rEM, one of rMD, and a final rEM refinement. Each rEM consisted of 500 iterations with application of conjugate gradients. Between the first two steps, the distance restraint force constant was increased from 1 to 2 kcal mol^{-1} Å^{-2}.

The rEM and rMD refinements were performed using skewed biharmonic penalty functions for the applied restraints. The calculations were performed in a vacuum, employing the

Table I: Equilibrium Binding Affinities Presented as IC_{50} Values on Displacement of [^{125}I]Monoiodo-Tyr^{26}-porcine Galanin (0.2 nM) for Galanin Receptors and of [^{3}H]Porcine NPY (0.1 nM) for NPY Receptors

peptide	IC_{50} (nM) galanin[a] receptor	IC_{50} (nM) NPY[b] receptor
galanin, porcine	0.8 ± 0.1	>10 000
galanin(1–13)	150 ± 20	>10 000
NPY, porcine	>10 000	1.0 ± 0.1
NPY(25–36)amide	>10 000	>1000[c]
galanin(1–12)–Pro–NPY(25–36)amide, M32	0.1 ± 0.02	250 ± 30
galanin(1–12)–Ala–NPY(25–36)amide	1.1 ± 0.2	100 ● 20

[a] Galanin binding was measured in membranes from rat hypothalamus. [b] NPY binding was measured in membranes from rat cerebral cortex. [c] Abens et al. (1989).

AMBER force field (Weiner et al., 1984), using charge reduction to 0.2 units (Lee et al., 1989) of the N-terminal amino group and of the guanidino groups of Arg residues. This charge reduction was introduced to prevent improper salt bridge formation. A distance-dependent dielectric function was used, $\epsilon = r_{ij}/r_0$ with distances in Å and $r_0 = 1$ Å (1 Å = 0.1 nm), in order to partially account for the dielectric screening by the solvent. The dihedral ω angles were restrained to ±180° using a force constant of 20 kcal mol^{-1} rad^{-2} throughout the refinement calculations (Lee et al., 1989). The force constants of the dihedral ϕ-angle restraints were 5 kcal mol^{-1} rad^{-2}. After the distance geometry calculations and before the rEM and rMD calculations, the C-terminal end of the polypeptide was amidated.

The rMD was preceded by an equilibration of 1 ps, which was initiated by assigning each atom an initial velocity at random from a Maxwell–Boltzmann distribution corresponding to 300 K. During the equilibration, scaling of atom velocities was carried out whenever the temperature difference between the instantaneous and specified temperatures exceeded 10 °C. During the rMD of 30 ps the system was loosely coupled to a thermal bath at 300 K (Berendsen et al., 1984) using a temperature relaxation time of 0.1 ps. The equilibration and rMD were performed using a time step of 1.0 fs in the Verlet leapfrog integration algorithm (Verlet, 1967).

When snapshots were extracted during the rMD run or at the end, they were subjected to a final rEM using the same force constants as in the rEM step just before the rMD. In the rEM steps as well as in the rMD, the effective nonbond interaction range was 11 Å and the distance within which the nonbond interaction decreased from the noncutoff value to 0 was 1.5 Å. The neighbor list for nonbond interactions was updated every 20 fs.

RESULTS

Receptor Binding Results

The equilibrium binding data on the studied peptide ligands at galanin receptors from rat hypothalamus and NPY receptors from rat cerebral cortex are presented in Table I. It is obvious that the chimeric peptide M32, i.e., galanin(1–13)–NPY-(25–36)amide, is a high-affinity ligand at both galanin and NPY receptors (with $IC_{50} = 0.1$ and ~250 nM, respectively) (Table I). Another chimeric peptide, which is an analogue of M32 where Pro13 is replaced by Ala, showed in comparison with M32 a 10-fold lower affinity to the galanin receptor but displaced [^{3}H]NPY slightly better than M32 (Table I).

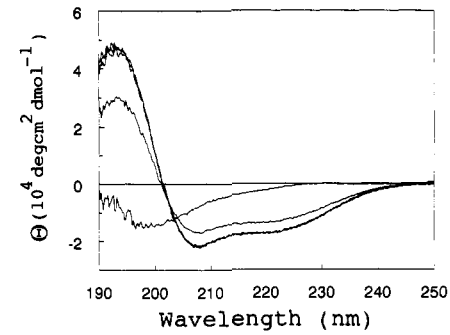

FIGURE 1: CD spectra of M32 in 0, 10, 20, 30, and 40% (v/v) 1,1,1,3,3,3-hexafluoro-2-propanol at pH 3.1 and 22 °C. From the top at 222 nm, the 0%, 10%, and coinciding 20, 30, and 40% spectra are shown. Mean residual ellipticities are used.

The separate galanin portion of M32, galanin(1–13), is not a ligand at NPY receptors, and the NPY portion of M32, NPY(25–36)amide, is not a ligand at galanin receptors.

CD Results

The CD spectra of M32 at pH 3.1 and 22 °C and in different concentrations of the cosolvent 1,1,1,3,3,3-hexafluoro-2-propanol are displayed in Figure 1. With the negative ellipticity at 222 nm as a measure of the α-helix content we see directly that in water there is hardly any α-helix developed at all, whereas at 10% (v/v) cosolvent there is already a considerable amount of α-helix formed. The three curves at 20, 30, and 40% (v/v) cosolvent practically coincide, demonstrating that a maximum of α-helix content is obtained at and above 20% (v/v) cosolvent. The ellipticity at 222 nm was transformed into a number of amino acid residues participating in α-helical conformation by using the mean residual contribution of −35 700 deg cm^2 dmol^{-1} for α-helix and 3900 deg cm^2 deg mol^{-1} for random coil (Greenfield & Fasman, 1969). At 30% (v/v) 1,1,1,3,3,3-hexafluoro-2-propanol we calculate that on the average 13.4 amino acid residues are engaged in α-helix formation. Thus, this condition, which yields a defined amount of α-helix in the peptide, was taken as suitable for the NMR investigation. We have found the same condition to apply for other peptides with a propensity to form α-helix, in particular NPY and NPY analogues and fragments (K. Arvidsson and A. Ehrenberg, unpublished results) and cecropin type peptides (Sipos et al., 1991, 1992). In addition, this mixture of H_2O and 30% (v/v) 1,1,1,3,3,3-hexafluoro-2-propanol may be assumed to simulate conditions at the surface of a lipid membrane.

The solution structure of galanin has been investigated by NMR and CD both in 30% (v/v) 1,1,1,3,3,3-hexafluoro-2-propanol (K. Arvidsson et al., unpublished results) and in 100% 2,2,2-trifluoroethanol (Wennerberg et al., 1990). Therefore, we performed CD measurements on the M32 chimeric peptide also in 100% 2,2,2-trifluoroethanol, for which condition we found 17.0 amino acid residues to be involved in α-helix formation. The increase from 13.4 α-helix-forming residues in 30% (v/v) 1,1,1,3,3,3-hexafluoro-2-propanol to 17.0 in 100% 2,2,2-trifluoroethanol for M32 should be compared with 8.2 and 12.9 α-helix-forming residues in the same two solvents, respectively, determined by us for rat galanin, which consists of 29 residues (K. Arvidsson et al., unpublished results). In both peptides 100% 2,2,2-trifluoroethanol promotes 15% more of the total sequence into α-helix

Table II: Proton NMR Chemical Shifts Recorded at 15°C, and $^3J_{HN\alpha}$ Spin–Spin Coupling Constants Recorded at 30 °C, of M32 in H_2O with 30% (v/v) 1,1,1,3,3,3-Hexafluoro-2-propanol and 10% ^2H_2O at pH 3.1

	chemical shift of proton (ppm)					coupling constant,
residue	NH	$C^\alpha H$	$C^\beta H$	$C^\gamma H$	other	$^3J_{HN\alpha}$ (Hz)
Gly1		3.83				
		3.93				
Trp2	8.52	4.77	3.32		2H 7.26, 4H 7.63, 5H 7.16	
					6H 7.24, 7H 7.46, NH 9.57	
Thr3	7.87	4.41	4.30	1.20		7.9
Leu4	7.87	4.13	1.61	1.61	$C^\delta H_3$ 0.87	5.5
Asn5	8.02	4.65	2.83		$N^\delta H_2$ 6.72, 7.43	
Ser6	8.04	4.37	3.93			6.1
Ala7	8.10	4.19	1.49			4.4
Gly8	8.16	3.80				
Tyr9	7.68	4.39	3.17		2,6H 7.18, 3,5H 6.87	4.8
Leu10	7.83	4.26	1.86	1.67	$C^\delta H_3$ 0.90	6.0
Leu11	8.16	4.32	1.86	1.75	$C^\delta H_3$ 0.88	6.3
Gly12	8.08	4.07				
		4.22				
Pro13		4.41	2.03	2.07	$C^\delta H_2$ 3.71, 3.80	
			2.44	2.22		
Arg14	7.80	4.07	1.92	1.71	$C^\delta H_2$ 3.19, $N^\epsilon H$ 7.10	5.0
His15	8.33	4.43	3.36		2H 8.32, 4H 6.98	6.9
Tyr16	7.96	4.27	3.11		2,6H 7.11	8.0
			3.22		3,5H 6.84	
Ile17	8.47	3.81	1.96	1.34	$C^\gamma H_3$ 0.98	6.2
				1.81	$C^\delta H_3$ 0.92	
Asn18	8.14	4.43	2.83		$N^\delta H_2$ 6.59, 7.40	
			3.03			
Leu19	7.81	4.13	1.86	1.67	$C^\delta H_3$ 0.90	5.2
Ile20	8.47	3.81	1.88	1.18	$C^\gamma H_3$ 0.88	6.2
				1.55	$C^\delta H_3$ 0.78	
Thr21	8.17	4.04	4.42	1.40		4.2
Arg22	7.91	4.18	2.05	1.81	$C^\delta H_2$ 3.19, $N^\epsilon H$ 7.23	6.5
Gln23	8.19	4.16	2.23	2.49	$N^\epsilon H_2$ 6.49, 7.02	
Arg24	8.18	4.14	1.71	1.38	$C^\delta H_2$ 3.01, 3.09	5.3
			1.76		$N^\epsilon H$ 7.03	
Tyr25	8.05	4.62	2.96		2,6H 7.28	7.3
			3.28		3,5H 6.87	
amide	7.00					
	7.35					

compared with the effect of 30% (v/v) 1,1,1,3,3,3-hexafluoro-2-propanol.

All CD measurements were made at 22 °C, while NMR data from which the structure is calculated, *vide infra*, were collected at 15 °C. For other peptides studied in the same solvent, 30% (v/v) 1,1,1,3,3,3-hexafluoro-2-propanol, a comparatively small increase in the α-helix content was found when reducing the temperature from 22 to 15 °C as derived from CD measurements. For NPY with 36 residues the temperature dependence of α-helix content is 0.06 residue per degree (K. Arvidsson and A. Ehrenberg, unpublished results), for the 22-residue motilin it is 0.05 residue per degree (A. Gräslund, personal communication), and for porcine cecropin with 31 residues it is 0.15 residue per degree (Sipos et al., 1992). Since the α-helix is located essentially in the NPY-derived portion of peptide M32, *vide infra*, we may assume the temperature dependence to be similar to that of NPY itself and calculate the α-helix content at 15 °C to be 13.8 residues.

NMR Results

Assignments. After examination of initial 2-D NMR experiments at several temperatures, it was decided that 15 °C was a suitable compromise, considering peptide flexibility at higher temperatures and line broadening at lower temperatures. Furthermore, at 15 °C no cross peaks were hidden in the H_2O resonance. The H_2O resonance was found to move upfield 0.01 ppm/°C in the solution of 30% (v/v) 1,1,1,3,3,3-hexafluoro-2-propanol. This temperature dependence is close to the value of 0.012 ppm/°C for neat water (Basus, 1989).

The sequence-specific (Wüthrich, 1986) and main-chain-directed (Englander & Wand, 1987) assignment methods were both found to be useful in the resonance assignment procedure of the peptide.

Some chemical shift degeneracies (see Table II) caused ambiguities in the assignment of two NOESY cross peaks. One of these had the alternative assignments of $d_{\alpha N}(8,12)$ and $d_{N\delta}(12,13)$. The other ambiguity had the alternative assignments of $d_{\alpha\delta}(12,14)$ and the intraresidual $d_{\alpha\delta}$ of Arg14. Neither changing the temperature from 15 to 50 °C nor changing the pH from 3.1 to 4.2 helped to resolve these ambiguities. The requirement that a correct NOESY assignment should be compatible with a structure giving low target function values and small restraint violations in the structure calculation (Havel, 1991) was used to distinguish between the alternative assignments. The DIANA calculations suggested the assignment alternatives $d_{N\delta}(12,13)$ and $d_{\alpha\delta}(12,14)$, respectively.

Chemical Shifts. The chemical shifts of assigned proton resonances of M32 in 30% (v/v) 1,1,1,3,3,3-hexafluoro-2-propanol at 15 °C and pH 3.1 are compiled in Table II together with the spin–spin coupling constants, $^3J_{HN\alpha}$.

It has been demonstrated (Clayden & Williams, 1982; Pastore & Saudek, 1990) that the chemical shift of the $C^\alpha H$ proton resonance is sensitive to the local secondary structure. In particular a large upfield shift relative to the random-coil

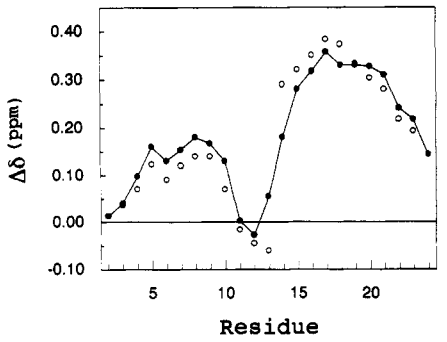

FIGURE 2: Upfield chemical shift differences for the C$^{\alpha}$H proton resonances relative to random-coil values (Wüthrich, 1986), averaged over $n \pm 1$. Filled circles denote M32 at 15 °C. Open circles denoted galanin(1–16) at 30 °C for residues 1–13 and NPY at 30 °C for residues 14–25. All shift data were recorded in 30% (v/v) 1,1,1,3,3,3-hexafluoro-2-propanol.

values over a succession of residues suggests the presence of an α-helix. Disturbing local effects may be filtered out by taking the average of the shift values of each amino acid residue and its nearest neighbors (Pastore & Saudek, 1990). A plot of such data for M32 is shown in Figure 2. The strong upfield shift in the NPY region of the peptide (i.e., amino acid residues 14–25) suggests the presence of an α-helix in the section of residues 14–24, approximately. Residues 11-13 are not structured. A weak tendency for α-helix formation may be present in the sequence of residues 5–10.

In Figure 2 comparison is also made with shift data (K. Arvidsson, K. Chandrasekhar, and A. Ehrenberg, unpublished results) for a galanin segment, galanin(1–16), and for NPY, both in the same solvent of 30% (v/v) 1,1,1,3,3,3-hexafluoro-2-propanol as used for M32. Apparently the α-helix-forming capacity is very similar in the corresponding sections of these parent peptides compared to those of M32. Only at the joining point of the two segments of the chimeric peptide, i.e., for residues Pro13 and Arg14, are there significant discrepancies.

We have also calculated similar upfield shift differences for galanin in 2,2,2-trifluoroethanol using published data (Wennerberg et al., 1990). These shift differences (not shown) practically coincide with those of the hybrid M32 over its galanin-derived segment. The other half, the carboxylate end of galanin, shows a somewhat larger tendency for α-helix formation than the amino end, but judged from the shift differences, the α-helix stability in that section of galanin in 2,2,2-trifluoroethanol is considerably smaller than for the NPY section of M32 in 30% (v/v) 1,1,1,3,3,3-hexafluoro-2-propanol.

We have also used similarly averaged shift changes for M32 at different temperatures in order to study how the α-helix stability changes with temperature. The shift values were determined at three temperatures, and the $n \pm 1$ averages of the shift changes in the temperature intervals 15–30 °C and 15–50 °C are plotted in Figure 3. This plot suggests that the α-helix is successively destabilized from the carboxy terminal as the temperature is increased.

Analysis of NOE Connectivities. The NOE connectivities are compiled in Figure 4. A clear sequence of d_{NN} connectivities from Arg14 to Ile20 combined with several medium-range $d_{\alpha N}(i, i+3)$ and $d_{\alpha\beta}(i, i+3)$ connectivities in the same region of the peptide suggest that these residues form an α-helix. This is in good agreement with the analysis of the C$^{\alpha}$H proton chemical shifts discussed above. The absence of any strong NOE connectivities over the sequence from Leu11 to Pro13 indicate lack of a defined structure in this region, which again agrees with the result of the chemical shift analysis. The two d_{NN} connectivities Gly8 to Tyr9 and Tyr9 to Leu10

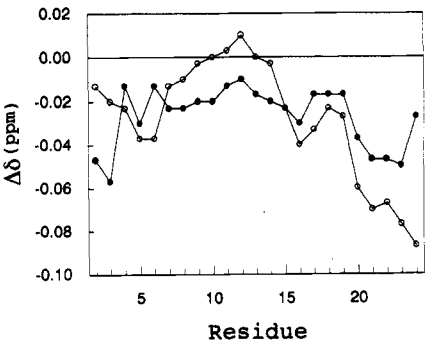

FIGURE 3: Upfield chemical shift changes with temperature for the C$^{\alpha}$H proton resonances of M32, averaged over $n \pm 1$. Filled circles denote the change from 15 to 30 °C, and open circles denote the change from 15 to 50 °C.

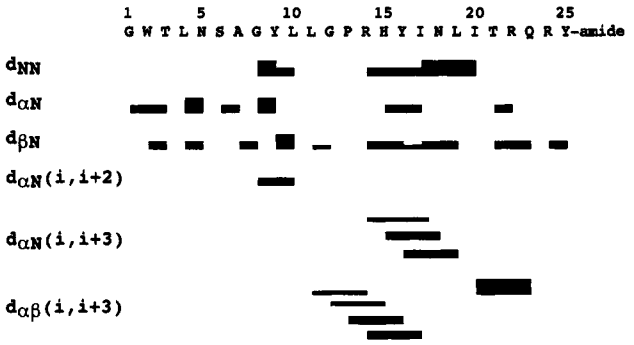

FIGURE 4: Amino acid sequence of M32 and survey of NOE connectivities of importance for the secondary structure in 30% (v/v) 1,1,1,3,3,3-hexafluoro-2-propanol at 15 °C. Thick, medium, and thin bars indicate strong, medium, and weak NOE connectivities, respectively.

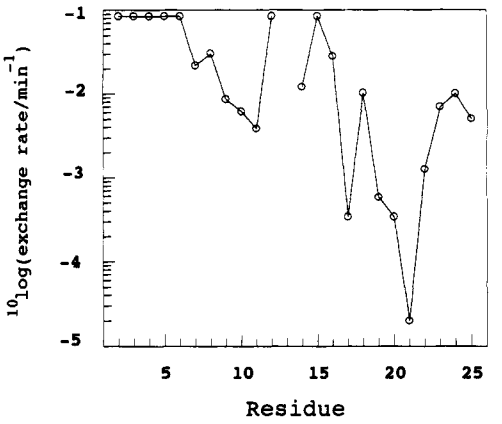

FIGURE 5: Backbone amide proton exchange rates of M32 in ^2H_2O with 30% (v/v) 1,1,1,3,3,3-hexafluoro-2-propanol at 15 °C, p^{2}H 3.3. The amide protons of Ile17 and Ile20 are treated as one proton and are given the same exchange rates because of coinciding chemical shifts and difficulties in fitting the exchange data to a double-exponential decay.

together with the clear $d_{\alpha N}(i, i+2)$ connectivity between Gly8 and Leu10 suggest the possibility that these residues form a reverse turn.

Backbone Amide Proton Exchange. Time series of peak intensities were extracted from slices through each fingerprint cross peak in the TOCSY experiments, recorded on a fresh ^2H_2O sample, p^{2}H 3.3. The amide proton exchange rates were calculated by fitting each such time series to a single-exponential decay by nonlinear regression. These amide proton exchange rates, plotted in Figure 5, show two separated regions of amino acid residues with reduced amide proton exchange

rates compared to expected values in random-coil structures (Wagner & Wüthrich, 1982).

The amino acid residues in the sequence from Ala7 to Leu11 all show exchange rates that are at least about 3–20 times lower than the ones calculated for the stretch from Trp2 to Ser6. For this latter stretch the amide proton exchange rates are ≥ 0.08 min^{-1}. These values are in fair agreement with the exchange rate of 0.055 min^{-1} determined by Wagner and Wüthrich (1982) for amide protons exposed to the solvent at 10 °C and p^{2}H 3.5. For the region from Arg14 to Tyr25 the exchange rate values are more inhomogeneous. The lowest exchange rates are those for Ile17, Leu19, Ile20, and Thr21, which have exchange rates at least 170–4000 times lower than the N-terminal stretch from Trp2 to Ser6. Noticeable is that the exchange rates in the C-terminal sequence from Arg22 to Tyr25 all are more than 1 order of magnitude lower than the ones in the N-terminus.

Calculation of Structures. A total of 112 nontrivial distance restraints were derived from assigned NOESY cross peaks and applied as input parameters for the DIANA structure calculations. Among these distance restraints, 64 were interresidual; of these, 48 were sequential and 16 were medium-range distances, out of which 29 and 9, respectively, are shown in Figure 4.

A total of 17 dihedral ϕ angles were determined from the measured $^3J_{HN\alpha}$ coupling constants shown in Table II. The restraint interval of these ϕ angles was chosen as ±20° in the region where chemical shifts and NOE connectivities, *vide supra*, suggested α-helical structure. In other regions where more flexibility must prevail, an extended interval of ±30° was used. The allowed interval for Ile17 and Ile20 was also ±30° because of overlapping NH–C$^\alpha$H COSY cross peaks. For Tyr9 the $^3J_{HN\alpha}$ value was even less accurate, so that an interval of ±35° was used.

The total number of dihedral angle restraints reached by the REDAC cycles was 98, of which 47 applied to the backbone of the polypeptide.

In total, 30 different structures were calculated by DIANA. From these structures, those 10 with the lowest value of the target function were selected and subjected to structure refinement as described in Materials and Methods. Frames during the last 10 ps of the 30-ps rMD indicated that no systematic changes in the energies occurred during this period. The structures at the end of the refinement procedure, after the final rEM, were ordered according to their energies. These ten "best or lowest energy" structures are in the following referred to as the NMR structures.

Backbone Hydrogen Bonds. Hydrogen bonds were searched for by defining an upper limit for the distance O···H of 2.40 Å and lower limits for the angles O···H–N and C–O···H of 135° and 110°, respectively (Åqvist et al., 1985). All three criteria should be fulfilled simultaneously.

In Figure 6 the backbone hydrogen bond patterns of the ten NMR structures are displayed. The structures are ordered from 1 to 10 according to increasing energy. Nearly all structures have a solid backbone NH(i)–CO($i-4$) hydrogen bond pattern including Pro13 (first CO($i-4$)) up to Ile20 (last NH(i)), proving that the NMR data define a stable α-helix in this part of the peptide.

For the two structures with lowest energy, the hydrogen bonds of this kind stretch from Pro13 to the C-terminal Tyr25. In the other eight structures, no hydrogen bonds involve the amide protons of residues 21–23, whereas there is a high frequency of (i,$i-3$) and (i,$i-4$) hydrogen bonds from Arg24 and Tyr25, respectively. These observations indicate that there

FIGURE 6: Overview of backbone hydrogen bonds detected in the ten NMR structures of M32. The structures are ordered according to increasing energy. Filled and open boxes denote NH(i)–CO($i-4$) and NH(i)–CO($i-3$) hydrogen bonds, respectively. Vertically and horizontally hatched boxes represent NH(i)–CO($i-5$) and NH(i)–CO($i-2$) hydrogen bonds, respectively. The hydrogen bond criteria are described in NMR Results, under Backbone Hydrogen Bonds. The donor NH is indicated by the index i. The amide proton of Tyr25 in structure no. 9 can be involved in either an (i, $i-3$) or an (i, $i-4$) hydrogen bond, of which only the latter has been shown.

is a tendency to elongate the α-helix to the C-terminus. Even when there is a bend at Ile20–Thr21, the following four residues still tend to form one turn of helix.

In all of the ten structures, backbone (i,$i-3$) or (i,$i-4$) hydrogen bonds from Tyr9 and Leu10 are found, confirming the capacity to form a reverse turn in this region. This finding, together with the number of (i,$i-4$) and (i,$i-3$) hydrogen bonds found over residues Thr3-Gly8, indicates a tendency to form α-helix over the sequence from Thr3 to Leu10. The reverse turn of Ser6-Tyr9 or Ala7-Leu10 and its surrounding behaves like a nascent helix.

In nine of the ten structures, backbone hydrogen bonds are bridging Pro13. On the other hand, only four bonds are found that bridge Gly12. This suggests that Pro13 does indeed participate in the α-helix and that Leu11 and Gly12 form a more flexible section.

Analysis of Secondary Structures. In Figure 7 the ten NMR structures are compared in the region of possible α-helix. A very good fit is obtained for all the structures over the range of residues 13–20 where a well-ordered α-helix is seen. Only Pro13 is slightly less well ordered in the α-helix. In two of the structures the α-helix is seen to extend to the C-terminal amino acid residue 25. It is also clearly seen that in the other structures there is a tendency for an α-helix turn after the bend at residues 20–21.

Figure 8 serves to illustrate the formation of a reverse turn of Ser6-Tyr9, or alternatively of Ala7-Leu10, or a nascent α-helix from Ser6 to Leu10.

Analysis of Backbone Dihedral Angles. Both ϕ and ψ dihedral angles should have well-defined values in a stable secondary structure. In a regular α-helix their values should be –57° and –47°, respectively. The ψ angles for the ten NMR structures are plotted in Figure 9. Before analyzing these data, it is important to point out that a change in the value of the angle ψ of an amino acid i changes the orientation of the following peptide bond, CO(i)–NH($i+1$), and the positions of all the following amino acid residues. In Figure 9 it is seen that the ψ values vary over the full turn for residues 2–5, whereas those of residues 1 and 6 are somewhat more restricted. For residues 7–10 the ψ angles are well defined with values compatible with a reverse turn or a nascent α-helix. There is some tendency of this structure to extend over the neighboring residues. The ψ values are ill-defined for residues 10–12, showing considerable flexibility in this section. The ψ angles are very well defined for residues 13–19. Over this section the average value of ψ is –48°, and for ϕ it is –57°,

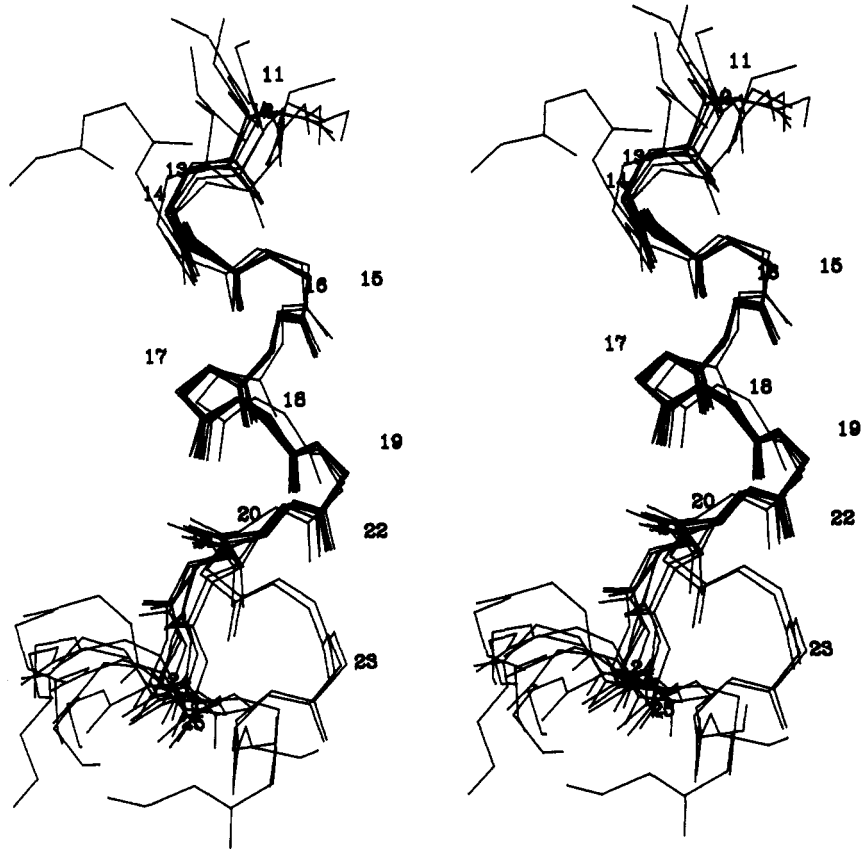

FIGURE 7: Superposition of amino acid residues 11–25 in the ten NMR structures of M32. The relative positions were found by minimizing the rmsd between the structure with lowest energy and each of the other ones over atoms C, $^{\alpha}$C, and N in amino acid residues 14–20.

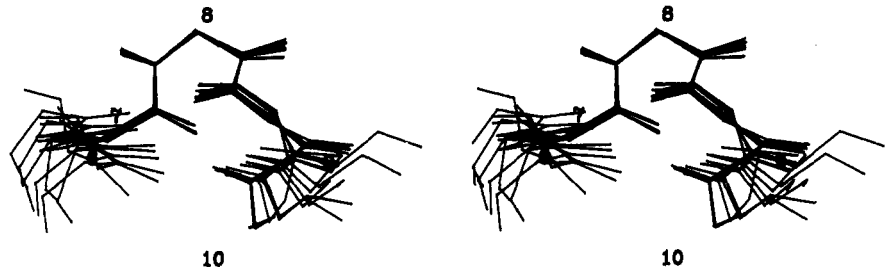

FIGURE 8: Superposition of amino acid residues 6–10 in the ten NMR structures of M32 in order to minimize the rmsd between the structure with lowest energy and each of the other structures over atoms C, $^{\alpha}$C, and N in amino acid residues 7–9.

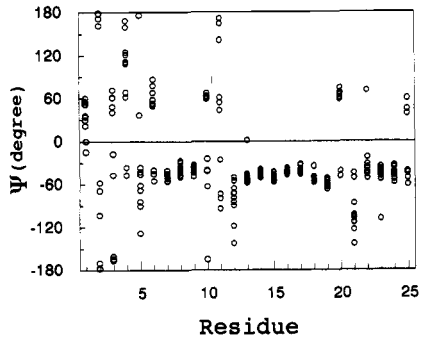

FIGURE 9: Backbone dihedral ψ angles in the ten NMR structures of M32.

in excellent agreement with the reference values of an α-helix. This α-helix is well defined from Pro13 to Ile20. From residue 20 to the C-terminus the ψ angle is less well defined again, but the variability is considerably smaller than in the N-terminal section. Calculated standard deviations for ψ of each residue, not shown, give similar information. The data of Figure 9 give additional information, however. They demonstrate for instance that there is a tendency toward a helix turn at the C-terminus, and in two of the structures the α-helix goes all the way from Pro13 to Tyr25. In Ile20 ψ seems to have a rather well defined alternative to the α-helix-compatible angle.

Contacts between Aromatic Side Chains. The peptide M32 contains four aromatic amino acid residues, Trp2 and Tyr9 in the galanin-derived part and Tyr16 and Tyr25 (a tyrosine amide) in the NPY-derived part. The possible approach and close contact between pairs of the aromatic rings of these side chains have been analyzed. Such information may be of importance in several ways. Trp2 is essential for the recognition of galanin by the galanin receptor, and in NPY, Tyr36 amide, corresponding to Tyr25 amide in M32, is essential for recognition and biological activity at NPY receptors. Interaction of these aromatic side chains with other aromatic groups might have an effect on receptor binding and activation. Both tryptophan and tyrosine residues may be studied by means of fluorescence. When fluorescence quenching and excitation transfer between such amino acid residues are analyzed, it is essential to know how close the aromatic

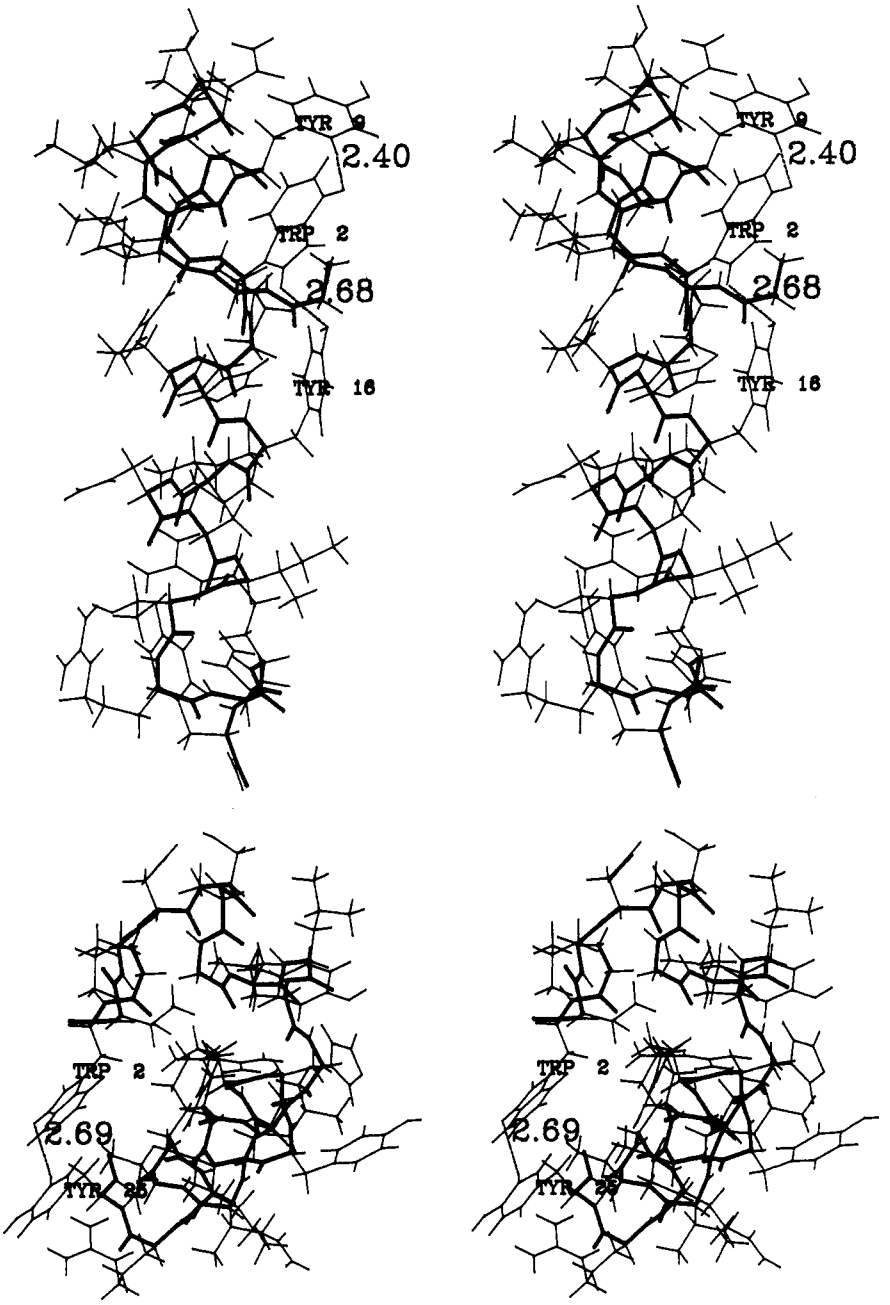

FIGURE 10: Structures of M32 having aromatic side chains in proximity to each other, with shortest distances between their ring protons shown in Å units. (A, top) One of the NMR structures in which Trp2 is close to both Tyr9 and Tyr16. (B, bottom) Close proximity between Trp2 and Tyr25 in another NMR structure.

groups might approach each other, since the effects on the fluorescence properties are sharply distance-dependent. Furthermore, reactive sites on aromatic side chains may be potential targets for synthetic bridges with the aim to stabilize a certain structure in a more rigid form.

Two of the ten NMR structures are shown in Figure 10 with all side chains included and the distances of close approach between aromatic side chains shown in Å units. Figure 10A shows a structure in which Trp2 is in proximity to Tyr9 and Tyr16 at the same time. Because of the flexibility at Gly12 and the nascent α-helix of residues 6–10, the N-terminal may be folded in such a way as to permit Trp2 to come close even to the C-terminal Tyr25 side chain when the bend at Ile20 and Thr21 gives proper folding. Such a case is shown in Figure 10B. In none of the structures have we found a close contact between Tyr9 and Tyr16.

Is the population of conformations of M32 with aromatic side chains in proximity to each other large enough to permit NOE to develop between protons in the different side chains? In order to increase the possibility of detecting and resolving long-range NOEs, a NOESY and a ROESY experiment were performed at 30 °C and 600 MHz, with mixing times of 125 and 60 ms, respectively. Another ROESY experiment was performed at 15 °C and 400 MHz, with a mixing time of 60 ms. However, no new medium- or long-range NOEs, in particular between aromatic side chains, could be detected in these spectra as compared with the previous NOESY results at 15 °C and 400 MHz. In addition, this indicates that the relevant correlation times for M32 under these conditions are larger than $\tau_c = 0.4$ ns.

Side-Chain Hydrogen Bonds. Analysis of the distances and bond orientations of the structure shown in Figure 10B suggests that hydrogen bonds may be formed between the

side chain of His15 and the carbonyl of Tyr9 as well as between the side-chain amide group of Asn18 and the carbonyl of Gly1. Such hydrogen bonds could help to stabilize a bent structure of the kind discussed.

In another of the ten NMR structures we have observed that the α-carbons of Gly1 and Tyr25 are fairly close to each other, at a distance of approximately 5Å, whereas the aromatic side chains of Trp2 and Tyr25 point in different directions and are further apart. This type of bent structure may be stabilized by a hydrogen bond between the side chains of Arg14 and Thr3.

DISCUSSION

The equilibrium binding data on M32 (Table I) show that M32 is recognized with high affinity by galanin receptors. Elongation of galanin(1–13) with NPY(25–36)amide increases the affinity 1000-fold, corresponding to a 4–5 kcal/mol increase in the free energy of binding (Table I). This suggests that eitner the NPY portion of M32 binds to galanin receptors or M32 adopts a specific structure because of intramolecular rearrangements causing additional interactions to occur between the receptor and the galanin(1–13) portion of M32. Similarly, the data on the displacement of [^{3}H]-NPY (Table I) show that M32 binds to the NPY receptors with an IC_{50} of 0.25 μm. The NPY(25–36)amide fragment, which constitutes the C-terminus of M32, has a much lower affinity, with an $IC_{50} > 1.0$ μM (Abens et al., 1989). Thus even recognition of the sequence of NPY(25–36)amide is enhanced by the presence of and interactions with galanin-(1–13), the N-terminal part of the chimeric peptide. It should be noted that the chimeric peptide M32 retains both NPY and galanin receptor recognition properties and thus acts as a bireceptor-recognizing peptide. Similarly, we found earlier that combining galanin(1–13) as N-terminus with substance P(5–11) as C-terminus resulted in another chimeric bireceptor-recognizing ligand, M15 (Bartfai et al., 1991; Lindskog et al., 1992), whose abilities to be recognized by both substance P and galanin receptors (Langel et al., 1992) were retained while the affinity for each of these was increased compared to their congeners.

The CD spectra of M32 in mixtures of water and 1,1,1,3,3,3-hexafluoro-2-propanol show that, with 30% (v/v) of this cosolvent, on the average 13–14 of the 25 amino acid residues are involved in formation of α-helix. The NMR results show that an extended α-helix portion is present in the NPY part of the chimeric peptide, just as in NPY itself where the C-terminal portion of residues 13–36 has α-helical character. In rat galanin the C-terminal stretch (a portion which is not present in M32) has some α-helix character, though significantly less than found for the C-terminal part in either M32 or NPY, as inferred from the analysis of the chemical shift differences. From the chemical shift studies, compiled in Table II and Figure 2, we obtained a clear indication that residues 14–24 of M32 participate in α-helical conformation, while residues 11–12 and 1–4 are not structured. Some weak α-helical character may be present in residues 5–10.

The ten final NMR structures, obtained after DIANA calculations and following rEM and rMD refinements, were examined for H-bond localization in the backbone (Figure 6), and the dihedral ψ angles were analyzed (Figure 9). These data show a well-developed α-helix between CO in Pro13 and NH in Ile20. Furthermore, the data reveal flexibility for Ile 20 and Thr21 followed by one turn of a C-terminal helix comprising residues Thr21 through Tyr25. These structural regions together with the reverse turn or nascent α-helix found in the region from Ser6 to Leu10 (Figure 8) add up to a total α-helical character in good agreement with the results of the CD measurements.

The measured backbone amide proton exchange rates presented in Figure 5 support the above conclusions about the structure. All amide protons suggested by the NMR structures to have a large tendency to be engaged in H-bond formation, i.e., those of residues Tyr9, Leu10, Ile17, Asn18, Leu19, Ile20, and Tyr25, are found to have low exchange rates. There are amide protons indicated to have some, but less, tendency to form H-bonds (Figure 6) which also have low exchange rates (Figure 5). These are amide protons of Leu11, Thr21, Arg22, Gln23, and Arg24. In particular, Thr21 shows a first-order exchange rate of 2×10^{-5} min^{-1}, which is remarkably low for a peptide. We cannot see any obvious structural reason for this very low rate. However, a possibility would be that the cosolvent molecules of 1,1,1,3,3,3-hexafluoro-2-propanol form solvation clusters around parts of the peptide in a way that hinders the access of water molecules to the backbone amide protons. This could also be a mechanism for the well-known effect of this cosolvent to stabilize α-helix structures, and Thr21 indeed occurs in such an α-helical portion of M32.

The NMR structures were also analyzed with respect to how close to each other the side chains of the aromatic amino acids could be situated. In particular it was found that Trp2 could be in close proximity to the C-terminal Tyr25 (Figure 10B). In another NMR structure the side chain of Trp2 is situated so that it has contact with both Tyr9 and Tyr16 (Figure 10A). Since the peptide M32 is flexible in the sections of residues 1–5, 11–12, and 20–21, the possibility of contact between the N- and the C-terminus is a dynamic property under the conditions of the NMR investigation. The conclusion is that the NMR structure with the side chains of Trp2 and Tyr25 in proximity to each other is one out of a great number of structures with equally low energy. Only a fraction of all the structures of M32 populated in solution will have the N- and the C-terminus close to each other. Under suitable conditions at a binding site such a folded structure of M32 may, however, be stabilized by interactions with the lipids of the membranes and the surface groups of the receptor. Such a folded structure, e.g., the one shown in Figure 10B, is reminiscent of the structure of NPY (or aPP), in which the N-terminal aromatic amino acid Tyr1 (Gly1 in aPP) may come into proximity to the C-terminal Tyr36, according to the X-ray crystallography structure of aPP (Blundell et al., 1981).

For NPY and the related bPP, some NMR experiments show solution structures stabilized in a conformation with the two termini close to each other (Darbon et al., 1992; Li et al., 1992), while in other experiments no such stabilization was found (Saudek & Pelton, 1990; Cowley et al., 1992; Mierke et al., 1992; K. Arvidsson et al., unpublished results). Whether the back folding is stabilized or not seems to be dependent on the solvent conditions. We have in the case of M32 and the particular solvent used looked very carefully for any NOE contacts revealing stabilization of a back-folded structure. For this purpose we utilized the increased sensitivity at the proton frequency of 600 MHz, which in our experiment gave an improvement by a factor of 4–5 in signal-to-noise ratio, but no new NOE contacts could be found, compared to data collected at 400 MHz.

With NPY it has been demonstrated that one receptor subtype requires both the N- and the C-terminus of NPY for recognition (Schwartz et al., 1989; Wahlestedt et al., 1990; Rivera & Undén, 1990; McLean et al., 1990). In addition

it has been shown that bridged and centrally truncated derivatives of NPY, where the remaining terminal stretches of amino acid residues are locked in proximity to each other, retain high affinity and high activity in systems containing this receptor subtype (Beck et al., 1989; Krstenansky et al., 1989; McLean et al., 1990). It should be of interest to examine analogous derivatives of M32.

In summary, it appears that the α-helix-forming propensity of the sequence NPY(25–36)amide is strongly expressed in the structure of M32. The other section of M32, i.e., galanin-(1–13), is essentially flexible but also adopts the structural feature of a nascent α-helix or a reverse turn. These properties enable the N-terminus to come into contact with the C-terminal α-helix. M32 is recognized by both galanin and NPY receptors, suggesting that it has preserved motifs which were present in the endogenous galanin and NPY molecules, respectively.

Recently we synthesized a chimeric peptide analogue to M32, galanin(1–12)–Ala–NPY(25–36)amide, which acts as a high-affinity galanin receptor ligand (cf. Table I) and is also recognized by NPY receptors from the rat cerebral cortex. An analysis of the structure of this analogue of M32 is underway.

Preliminary pharmacological findings (Z. Wiesenfeld-Hallin et al., in preparation) show that the chimeric peptide M32 not only is a high-affinity ligand at both galanin and NPY receptors but also may act as an antagonist of galanin action. In the present study we have provided models of possible solution structures of M32. Understanding of the secondary and tertiary structure of this interesting peptide receptor antagonist may shed light on agonist/antagonist discriminations at peptide receptors.

ACKNOWLEDGMENT

We wish to thank Dr. Anders Karlström at Kabi Pharmacia Biopharma for kindly letting us use the CD spectropolarimeter. The Swedish NMR Centre, Stockholm, is acknowledged for giving us permission to use the Varian Unity 600 spectrometer, and Dr. Toshi Nishida and colleagues are thanked for friendly assistance. We are grateful to Mr. Torbjörn Astlind for skilled assistance with computers and programs. Mrs. Haidi Astlind is acknowledged for patiently operating the word processor.

SUPPLEMENTARY MATERIAL AVAILABLE

Two tables of data used as input for DIANA calculations, one with NOE intensities from which nontrivial upper limit distances were calculated and one showing dihedral ϕ ranges; one table with coordinates of the atoms of the ten NMR structures (70 pages). Ordering information is given on any current masthead page.

REFERENCES

Abens, J., Undén, A., Andell, S., Tam, J. P., & Bartfai, T. (1989) in *Neuropeptide Y* (Mutt, V., Fuxe, K., Hökfelt, T., & Lundberg, J. M., Eds.) pp 137–142, Raven Press, New York.

Allen, J., Novotny, J., Martin, J., & Heinrich, G. (1987) *Proc. Natl. Acad. Sci. U.S.A. 84*, 2532–2536.

Åqvist, J., van Gunsteren, W. F., Leijonmarck, M., & Tapia, O. (1985) *J. Mol. Biol. 193*, 461–477.

Bartfai, T., Bedecs, K., Land, T., Langel, Ü., Bertorelli, R., Girotti, P., Consolo, S., Xu, X., Wiesenfeld-Hallin, Z., Nilsson, S., Pieribone, V. A., & Hökfelt, T. (1991) *Proc. Natl. Acad. Sci. U.S.A. 88*, 10961–10965.

Bartfai, T., Fisone, G., & Langel, Ü. (1992) *Trends Pharmacol. Sci. 13*, 312–317.

Basus, V. (1989) *Methods Enzymol. 177*, 132–149.

Beck, A., Jung, G., Gaida, W., Köppen, H., Lang, R., & Schnorrenberg, G. (1989) *FEBS Lett. 244*, 119–122.

Berendsen, H. J. C., Postma, J. P. M., van Gunsteren, W. F., DiNola, A., & Haak J. R. (1984) *J. Chem. Phys. 81*, 3684–3690.

Blundell, T. L., Pitts, J. E., Tickle, I. J., Wood, S. P., & Wu, C.-W. (1981) *Proc. Natl. Sci. U.S.A. 78*, 4175–4179.

Bystrov, V. F. (1976) *Prog. Nucl. Magn. Reson. Spectrosc. 10*, 41–82.

Clayden, N. J., & Williams, R. J. P. (1982) *J. Magn. Reson. 49*, 383–396.

Cowley, D. J., Hoflack, J. M., Pelton, J. T., & Saudek, V. (1992) *Eur. J. Biochem. 205*, 1099–1106.

Darbon, H., Bernassau, J.-M., Deleuze, C., Chenu, J., Roussel, A., & Cambillau, C. (1992) *Eur. J. Biochem. 209*, 765–771.

Davis, D. G. (1989) *J. Magn. Reson. 81*, 603–607.

Eich, G., Bodenhausen, G., & Ernst, R. R. (1982) *J. Am. Chem. Soc. 104*, 3731–3732.

Englander, S. W., & Wand, A. J. (1987) *Biochemistry 26*, 5953–5958.

Fisone, G., Langel, Ü., Land, T., Berthold, M., Bertorelli, R., Girotti, P., Consolo, S., Crawley, J. N., Hökfelt, T., & Bartfai, T. (1991) in *Galanin: A New Multifunctional Peptide in the Neuro Endocrine System* (Hökfelt, T., Bartfai, T., Jacobowitz, D., & Ottoson, D., Eds.) pp 213–220, Macmillan Press, Cambridge.

Gozes, Y., Brenneman, D. E., Fridkin, M., Asofsky, R., & Gozes, I. (1991) *Brain Res. 540*, 319–321.

Greenfield, N., & Fasman, G. D. (1969) *Biochemistry 8*, 4108–4116.

Güntert, P., & Wüthrich, K. (1991) *J. Biomol. NMR 1*, 447–456.

Güntert, P., Braun, W., & Wüthrich, K. (1991) *J. Mol. Biol. 217*, 517–530.

Havel, T. F. (1991) *Prog. Biophys. Mol. Biol. 56*, 43–78.

Hoult, D. I., Chen, C.-N., Eden, H., & Eden, M. (1983) *J. Magn. Reson. 51*, 110–117.

Ishiguro, T., Fujita, S., Okano, R., Kato, N., Eguchi, C., & Matsuo, H. (1988) *Chem. Pharm. Bull. 36*, 2720–2723.

Karplus, M. (1959) *J. Chem. Phys. 30*, 11–15.

Kim, Y., & Prestegard, J. H. (1989) *J. Magn. Reson. 84*, 9–13.

Krstenansky, J. L., Owen, T. J., Buck, S. H., Hagaman, K. A., & McLean, L. R. (1989) *Proc. Natl. Acad. Sci. U.S.A. 86*, 4377–4388.

Land, T., Langel, Ü., Löw, M., Berthold, M., Undén, A., & Bartfai, T. (1991a) *Int. J. Pept. Protein Res. 38*, 267–272.

Land, T., Langel, Ü., Fisone, G., Bedecs, K., & Bartfai, T. (1991b) *Methods Neurosci. 5*, 225–234.

Langel, Ü., Land, T., & Bartfai, T. (1992) *Int. J. Pept. Protein Res. 39*, 516–522.

Lee, M. S., Gippert, G. P., Soman, K. V., Case, D. A., & Wright, P. E. (1989) *Science 245*, 635–637.

Li, X., Sutcliffe, M. J., Schwartz, T. W., & Dobson, C. M. (1992) *Biochemistry 31*, 1245–1253.

Lindskog, S., Ahrén, B., Land, T., Langel, Ü., & Bartfai, T. (1992) *Eur. J. Pharmacol. 210*, 183–188.

MacKerell, A. D., Jr. (1988) *J. Comput-Aided Mol. Des. 2*, 53–63.

McLean, L., Buck, S. H., & Krstenansky, J. L. (1990) *Biochemistry 29*, 2016–2022.

Mierke, D. F., Dürr, H., Kessler, H., & Jung, G. (1992) *Eur. J. Biochem. 206*, 39–48.

Nilges, M., Clore, M., & Gronenborn, A. M. (1988) *FEBS Lett. 239*, 129–136.
Pardi, A., Billeter, M., & Wüthrich, K. (1984) *J. Mol. Biol. 180*, 741–751.
Pastore, A., & Saudek, V. (1990) *J. Magn. Reson. 90*, 165–176.
Rivera, C. B., & Undén, A. (1990) *FEBS Lett. 277*, 23–25.
Saudek, V., & Pelton, J. T. (1990) *Biochemistry 29*, 4509–4515.
Schwartz, T., Fuhlendorff, J., Langeland, N., Thögersen, H., Jörgensen, J. C., & Sheikh, S. P. (1989) in *Neuropeptide Y* (Mutt, V., Fuxe, K., Hökfelt, T., & Lundberg, J. M., Eds.) pp 143–151, Raven Press, New York.
Sipos, D., Chandrasekhar, K., Arvidsson, K., Engström, Å., & Ehrenberg, A. (1991) *Eur. J. Biochem. 199*, 285–291.
Sipos, D., Andersson, M., & Ehrenberg, A. (1992) *Eur. J. Biochem. 209*, 163–169.
Sober, H. A., Ed. (1970) *Handbook of Biochemistry, Selected Data for Molecular Biology*, p B-75, CRC Press, Cleveland.
States, D. J., Haberkorn, R. A., & Ruben, D. J. (1982) *J. Magn. Reson, 48*, 286–292.
Tatemoto, K., Carlquist, M., & Mutt, V. (1982) *Nature 296*, 659–660.
Tatemoto, K., Rökaeus, Å., Jörnvall, H., McDonald, T., & Mutt, V. (1983) *FEBS Lett. 164*, 124–128.
Verlet, L. (1967) *Phys. Rev. 159*, 98–103.
Wagner, G., & Wüthrich, K. (1982) *J. Mol. Biol. 160*, 343–361.
Wahlestedt, C., Grundemar, L., Håkanson, R., Heilig, M., Shen, G. H., Zukowska-Grojec, Z., & Reis, D. J. (1990) *Ann. N.Y. Acad. Sci. 611*, 7–26.
Weiner, S. J., Kollman, P. A., Case, D. A., Singh, U. C., Ghio, C., Alagona, G., Profeta, S., Jr., & Weiner, P. (1984) *J. Am. Chem. Soc. 106*, 765–784.
Wennerberg, A. B. A., Cooke, R. M., Carlquist, M., Rigler, R., & Campbell, I. D. (1990) *Biochem. Biophys. Res. Commun. 166*, 1102–1109.
Wiesenfeld-Hallin, Z., Xu, X.-J., Langel, Ü., Bedecs, K., Hökfelt, T., & Bartfai, T. (1992) *Proc. Natl. Acad. Sci. U.S.A. 89*, 3334–3337.
Wüthrich, K. (1986) *NMR of Proteins and Nucleic Acids*, Wiley, New York.
Wüthrich, K., Billeter, M., & Braun, W. (1983) *J. Mol. Biol. 169*, 949–961.